Kenneth J. Hunt
and Juan Fang

13 A Morphological Viewpoint: Juxtaposition of Design Approaches for Locomotion-Rehabilitation Robotics

Abstract: *The Morphological Viewpoint: a morphological computation or control system is one which is designed from a morphological point of view.*

Introduction

Casual perusal of the literature on morphological computation reveals there is no widely-accepted formal definition of the term[1] although serious progress towards a formal theory is being made [6]. There are however several features of works which appear under this label. Usually, prominence is given to the shape, form or structure of the technical systems under consideration. These systems in turn are often related to robotics, and the interaction of these robots or robotic manipulators with human beings has a prominent role.

Our own field of professional activity is rehabilitation robotics and clinical applications for people with neurological impairments resulting from injury or disease. This focus further emphasises the importance of the interaction between the technical system and the human, because in this area the robotic system is usually designed to replace or augment some of the lost volitional function. It is attractive to begin the design process by having in mind the shape, form and structure of the correctly-functioning human system, and to shape the form of the technical support system to mimic or replace the parts of the human neuro-musculo-skeletal system which no longer work properly — this we might term a morphological approach. On the other hand, it is quite tempting to begin by formally specifying the functional requirements of the technical system and to proceed by building a solution which does not necessarily reflect in any direct way the human attributes of the system it is replacing or augmenting — some would say this represents a traditional engineering approach.

So, when is a system "morphological" and when is it not? Turning to more authoritative sources, the Oxford English Dictionary currently defines "morphology," in a scientific context, as *shape, form or external structure, especially of (a part of) an organism.* From this definition, one may boldly surmise that morphological computation, or a morphological control system, has quite a lot to do with shape, form and structure and that human beings (or other living things) are closely involved in using the technical systems which emerge: shape, form and structure are emphasised at the outset; the intended function of the system plays a secondary role initially. Morphology, perhaps, can be likened to an elephant: it is hard to define, but instantly recognisable when you see it.[2]

Attempts to find common ground in the definition of morphological computation are reminiscent of a debate which took place in the 1950s–60s regarding adaptive control, a hot topic of that era [1]. An apparently obvious definition at the time, and one which is prominent nowadays, is that to be adaptive, a feedback controller has to adapt its parameters or structure in response to changes in the controlled system. But then it was argued that even a time-invariant controller with fixed parameters can be considered adaptive because it adjusts its output in response to changes in the measurement of the controlled system's output or in the command signal. It is quite hard to imagine the latter type of controller as being adaptive, but you have to admit that it depends on the way you think about it. In fact, the issue was neatly resolved — some would

[1] Just try a database search using "morphological computation."
[2] The "elephant test."

say sidestepped — when the proposal was put forth that an adaptive control system is one which is designed from an adaptive point of view [11]. So, you can decide yourself whether the two types of controller described are adaptive or not because it depends on how you approach the technical problem at hand.

And so it might be with morphological computation and control, wherefore we propose:

> *The Morphological Viewpoint: a morphological computation or control system is one which is designed from a morphological point of view.*

At a basic level, it is useful to draw here on the formal definition of "morphology" given above, viz.: pertaining to shape, form or external structure, especially of (a part of) an organism.

In the sequel we will use a very simple rehabilitation robotics problem — the design and feedback control of an artificial ankle joint — to see what happens when one thinks in a morphological way (or otherwise).

Rehabilitation Robotics

Robotic systems intended for rehabilitation of walking, self-evidently, should come in a form that promotes and supports locomotion. It is challenging for patients with neurological impairments to walk, therefore gait rehabilitation robots have been developed to promote neurological rehabilitation, adaptation and recovery of function [10]. The physical shapes, or rather morphologies, of all dynamic systems influence their interaction with the environment [9]. Gait rehabilitation robots may initially be designed using morphological methods where effective physical shapes are determined. For example, a gait orthosis can have an exoskeleton connected by three revolute joints to mimic the lower limb. Although morphological design can lead to effective mechanical structures which allow walking, the target complex behaviours of locomotion, such as ankle plantarflexion and dorsiflexion, require engineering control [7]. Gait orthosis design thus adopts computing engineering methods based on morphological analysis and engineering control to achieve a smooth gait pattern.

Robotic devices are employed clinically for rehabilitation of people with paretic limbs [4]. For the lower limbs, several medically-certified products are available; these are used for rehabilitation of walking function in patients following a stroke, incomplete spinal cord injury, or in other neurological conditions. Prominent among these devices are the Lokomat[3] and G-EO[4] systems (Figure 1).

The Lokomat uses two rigid leg orthoses which have DC motors powering the knee and hip joints. The ankle joint is supported passively. The patient is attached to the orthoses and walks on a treadmill using the support of an overhead body-weight unloading system (Figure 1(a)). In the current version of the Lokomat, high-bandwidth feedback controls the knee and hip motors so that pre-programmed joint trajectories are followed. The operator is able to reduce the amount of guidance force so that deviation from

[3]Hocoma AG, Volketswil, Switzerland. www.hocoma.com
[4]Reha Technology AG, Olten, Switzerland. www.rehatechnology.com

(a) Lokomat. Picture: Hocoma AG, Switzerland.

(b) G-EO. Picture: Reha Technology AG, Switzerland.

Figure 1: *Robotic devices for rehabilitation of walking.*

the nominal gait pattern is permitted. In this way a certain amount of compliance is introduced and the patient has to start using volitional neuromuscular inputs to maintain an acceptable gait. This facet illustrates an important point which we will examine in more detail in the sequel (Sec.): the fact that a feedback control system for a robotics device is designed from a robust engineering perspective using high-performance DC motors does not preclude the possibility that the system can have features more readily thought to be associated with morphologically-designed components, e.g. characteristics of compliance and yielding.

The G-EO's principle of operation is different: it is an end-effector system in which the patient stands on two foot platforms which are driven by DC motors (Figure 1(b)). It is thus possible to achieve planar gait as well as simulated stair climbing and descent. The possibility of compliant behaviour is more obvious in this case since the trajectories of the feet can in principle be located anywhere in 2-D space.

The Lokomat and the G-EO systems both have the necessary attributes to be considered as morphological computation and control systems, but one would have to talk to the original design engineers at the Hocoma and Reha Technology companies to determine whether their design perspective was truly morphological . . . however that may be, it is certainly true that the Lokomat and the G-EO are solid engineering systems which exemplify the state of the art in rehabilitation robotics.

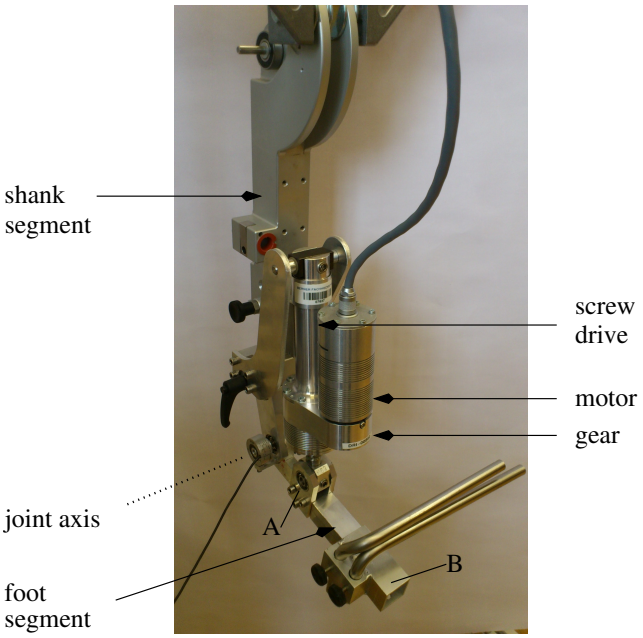

(a) Joint components. A DC motor is connected via gearing to a vertical screw drive. The drive applies a torque τ_{mj} to the foot segment at connection point A. In the experiments, an external disturbance torque d is applied manually at about point B. The ankle angle θ is measured by an analogue encoder positioned on the joint axis. Picture: K. J. Hunt.

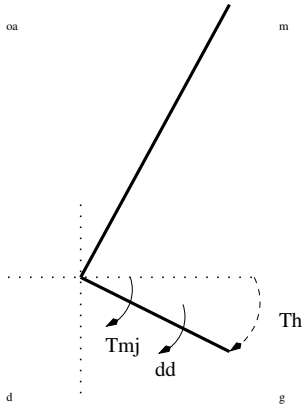

(b) Torques acting on the ankle joint: d is an external disturbance torque; τ_{mj} is a motor-generated torque acting on the joint after translation of the motor torque τ_m through a gearbox. The net ankle torque is $\tau = \tau_{mj} + d$.

Figure 2: *Artificial ankle joint for the Lokomat.*

Control of an Artificial Ankle Joint

The Lokomat product as currently marketed does not have actuation of the ankle joint but our lab has developed an artificial ankle joint which integrates with the existing leg orthoses (Figure 2). The form of the joint was chosen to mimic a simplified, planar human ankle joint. It is simplified in the sense that it exhibits only planar rotational motion and that it is driven by a single DC motor and gearbox which can produce both dorsiflexion and plantarflexion. The DC motor and gear assembly is the same as that used in the knee and hip joints of the Lokomat's orthoses.

The concepts under discussion will be elucidated using a simple feedback control loop we developed for the artificial ankle joint (Figure 3). Joint dynamics are often represented in the linear time-invariant form $J\ddot{\theta} = \tau - k_v\dot{\theta} - k_s\theta$, where θ is the angular deviation from an arbitrary neutral position and τ is the net joint torque. J is the moment of inertia while k_s and k_v represent the joint's intrinsic stiffness and viscous damping. These

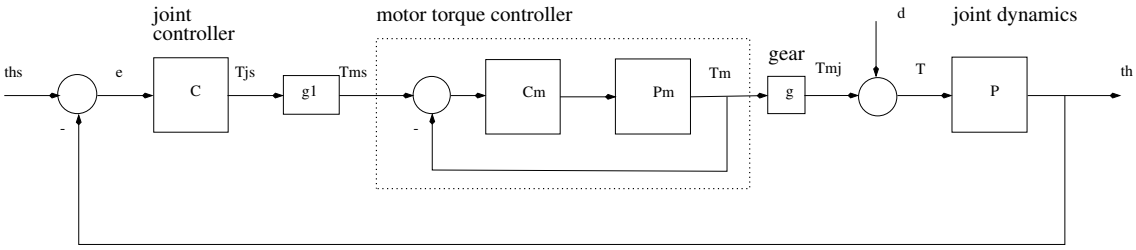

Figure 3: *Feedback loop for control of the artificial ankle joint. θ is the joint angle and θ^* its setpoint/reference value; the tracking error is $e = \theta^* - \theta$. The net joint torque is τ while d is an external disturbance torque. The motor-torque controller is internal to the DC motor control unit: it comprises a motor controller C_m acting on the motor plant P_m to keep the motor torque τ_m close to its reference value τ_m^*. τ_{mj} is the motor torque referred to the joint axis via gearing ratio g and τ_{mj}^* is its effective setpoint value.*

dynamics are represented as the transfer function P:

$$\tau \to \theta\text{:}\;\; P = \frac{1/J}{s^2 + \frac{k_v}{J}s + \frac{k_s}{J}}. \tag{1}$$

The ankle joint is driven by a DC motor[5] and gearing with ratio g which results in a torque τ_{mj} acting at the joint axis. The net joint torque comprises the motor-generated component, τ_{mj}, and an external disturbance torque d, i.e. $\tau = \tau_{mj} + d$ (Figure 2(b)); the angle and the moments acting on the joint are defined to be positive in a clockwise direction. The motor torque $\tau_m = \tau_{mj}/g$ is controlled to a reference torque τ_m^* using a feedback loop internal to the motor's control unit[6] (Figure 3); the torque controller is implemented internally as a current controller.

The ankle joint dynamics are modified by a linear time-invariant compensator with transfer function $C(s)$, which forms part of the feedback loop shown in Figure 3. Input to the compensator is the error signal e which is the deviation of the angle from a reference value θ^*: $e = \theta^* - \theta$. The compensator parameters will be determined here using simple impedance-like control strategies which aim to modify the joint's intrinsic stiffness and damping to alternative desired values. This means that, in contrast to model-based analytical control approaches, the parameters of the dynamic model P are not required for determination of the compensator parameters.

We proceed from the point of view that the compensator C is to be designed to achieve compliant ankle joint behaviour. In this view, the ankle joint should yield to the external disturbance torque d. One way of characterising this is to require the joint angle to respond to the disturbance in accordance with a pre-specified impedance law given by a desired closed-loop stiffness k_1 and damping k_2. Considering for simplicity steady-state conditions, our goal is to achieve a compliant joint response where the pliance is

[5] RE40 24 V, 150 W DC motor, Maxon Motor AG, Switzerland.
[6] ADS_E 50/10 servo amplifier, Maxon Motor AG, Switzerland.

characterised in steady state by the stiffness k_1. The joint position θ should then respond to a constant external disturbance torque d according to $d = k_1\theta \Leftrightarrow \theta = d/k_1$ as $t \to \infty$.

The key transfer function which can be used to analyse the compliance (or otherwise) of the closed-loop system is that describing the relationship between d and θ, known in control engineering circles as the load sensitivity function [2]:

$$d \to \theta\colon\ G_{\theta d}(s) = \frac{P(s)}{1 + C(s)P(s)}. \tag{2}$$

In steady state, i.e. $\omega \to 0$, assuming the plant to have low-pass behaviour, we have $|CP(j\omega)| \gg 1$. From Equation (2) it follows that the steady-state angle obtained in response to a constant disturbance torque (assuming for the moment a zero reference angle) is

$$\theta_{ss} \approx \lim_{\omega \to 0} |C(j\omega)|^{-1} d. \tag{3}$$

It turns out therefore that the steady-state compliance of the joint is related to the inverse of the compensator gain: the stiffness is then equivalent to the steady-state compensator gain $\lim_{\omega\to 0} |C(j\omega)|$.

A key design decision from a control engineering perspective is whether or not to include integral action in the compensator. For a Type-0 plant, i.e. a plant with no intrinsic integral action, the compensator will usually be designed with an integrator to eliminate steady-state reference-tracking error: with integral action the compensator has infinite gain at zero frequency so that any steady-state uncertainty is eliminated. But this is not what we want in the design of a compliant joint since the stiffness is then infinite and the compliance zero.

Turning back to our compliant way of thinking, therefore, we consider first the case when the compensator is designed as indicated above without integral action, e.g. a simple impedance controller $C(s) = k_1 + k_2 s$ having stiffness k_1 and damping k_2. In this case $\lim_{\omega\to 0} |C(j\omega)| = k_1$ and Equation (3) gives $\theta \approx \frac{1}{k_1} d \Leftrightarrow d \approx k_1\theta$: this reveals that the desired compliance is attained.

Now we consider a compensator with integral action, e.g. $C(s) = k_1 + k_2 s + \frac{1}{k_3 s}$, which results in $|C(j\omega)| \to \infty$ as $\omega \to 0$. This in turn, from Equation (3), leads to $\theta \approx 0$ (or the neutral position if the reference angle is non-zero). In this case the constant disturbance torque is countered by a motor-generated torque which forces the joint back to the neutral position and which in steady-state has the same magnitude as the disturbance torque. This control strategy is non-compliant because the compensator, with infinite steady-state gain, will always tend to drive the tracking error to zero by forcing the joint back to the neutral position as in Test 4 below (Figure 7).

One objection which might be raised at this point by a control engineer is that the compensator structures we have discussed up to now are non-proper. The compensator $C(s)$ is in general a transfer function in the complex variable s, which can be represented as $C(s) = \frac{G(s)}{H(s)}$ with G and H the numerator and denominator polynomials in s. From a practical perspective, it is usually important to make sure that C is strictly proper, i.e. $\deg G < \deg H$. This condition ensures the compensator gain rolls off at high frequency thus protecting the loop from the effects of high-frequency measurement noise:

when C is strictly proper, $\lim_{\omega\to\infty}|C(j\omega)| = 0$. This issue can easily be resolved with the impedance controller $C(s) = k_1 + k_2 s$ by adding to the damping term a low-pass filter with a bandwidth above the frequency of interest for closed-loop response characteristics but below the frequency range of any undesirable noise. In the situation discussed above, the desired stiffness and damping properties will be maintained in the frequency range relevant to the performance and behaviour of the joint.

Experimental Results

We designed a series of experiments with the artificial ankle joint in order to illustrate the concepts developed above. All experiments started at a neutral joint reference position of $\theta^* = 30$ deg. The joint was then moved as described below by the experimenter applying upward or downward forces at the end of the "foot" segment close to point B (Figure 2(a)). This manual intervention corresponds to the external disturbance torque d (Figs. 2 and 3).

In the first test, the controller was designed to give a compliant pure-stiffness characteristic with stiffness $k_1 = 2.4$ Nm/deg, no damping, $k_2 = 0$, and no integral action, $k_3 \to \infty$ (Figure 4). The result shows that the desired pure-stiffness behaviour was achieved almost exactly (Figure 4(b)) and that the behaviour was compliant: when moved to a position of approximately 20 or 40 deg, a constant joint moment is generated and the controller makes no further attempt to force the joint back to the neutral position (Figure 4(a), lower graph). The joint stiffness can be assessed using plots of the motor-generated joint torque against joint angle (e.g. Figure 4(b)) because in steady-state or slow-movement conditions the magnitude of the external disturbance torque applied to the joint must be approximately equal to the motor-generated torque τ_{mj}.

In the second test, damping was added to the controller by setting $k_2 = 1$ Nm·s/deg (Figure 5). The damping term $k_2 s$ was augmented as described above by a first-order low-pass filter with time constant 0.1 s, i.e. the filter transfer function was $\frac{1}{0.1s+1}$; without this filter, measurement noise from the angle sensor was amplified to an unacceptable degree. There is now substantial deviation from a pure-stiffness characteristic (Figure 5(b)) but the joint behaviour remains compliant since a constant joint torque is generated at the off-neutral positions of 20 and 40 deg (Figure 5(a), lower graph). The impedance characteristic is somewhat elliptical in shape and roughly symmetric around the line of constant stiffness (Figure 5(b)). The deviation from the dashed line of constant stiffness results from the damping component $k_2\frac{d\theta}{dt}$ generated during dynamic transitions between the two off-set-point angles of 20 and 40 deg.

The third and fourth tests were carried out with $k_1 = 2.4, k_2 = 0$ and with integral action in the compensator: k_3 was set to 4 deg·s/Nm. In the third test (Figure 6), the experimenter attempted to maintain a joint-angle profile similar to that used in tests 1 and 2. At the off-set-point angles of 20 and 40 deg the integral component acts on the constant set-point error and the motor-generated joint torque increases (Figure 6(a), lower graph). The experimenter had to gradually increase the torque applied manually in the opposite direction in order to match the increasing motor-generated torque and main-

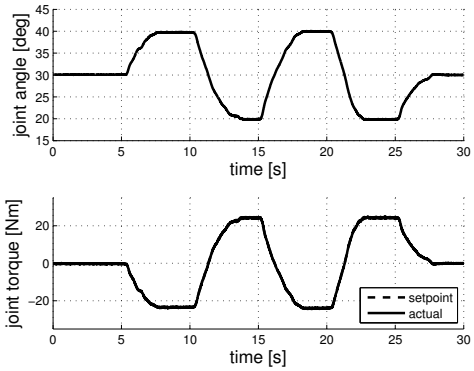

(a) Joint angle θ and torque τ_{mj}. In the lower graph, the setpoint curve is obscured by the data points.

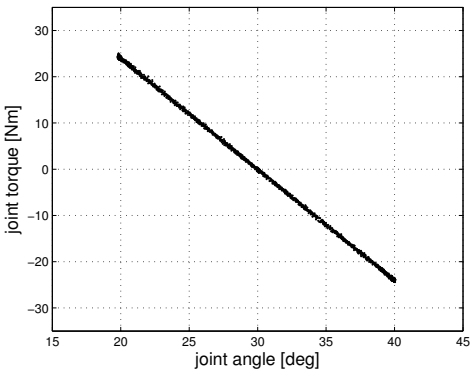

(b) Joint torque τ_{mj} vs. joint angle θ: pure stiffness characteristic of 2.4 Nm/deg (-ve slope of dashed line, partly obscured by data points).

Figure 4: *Test 1. Compliant behaviour with stiffness only: experimental results with $k_1 = 2.4$ Nm/deg (stiffness), $k_2 = 0$ (no damping) and $k_3 \to \infty$ (no integral action). The joint was manually moved between the angles of approximately 20 and 40 deg and held at these levels for a short time between moves.*

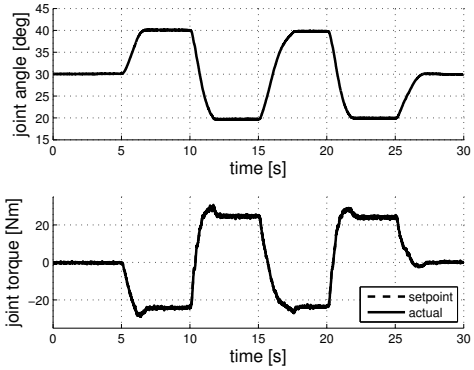

(a) Joint angle θ and torque τ_{mj}.

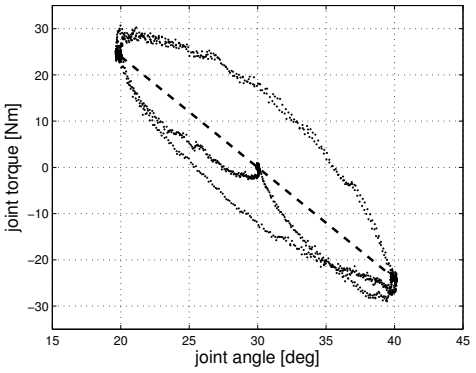

(b) Joint torque τ_{mj} vs. joint angle θ: clear deviation from a pure stiffness characteristic of 2.4 Nm/deg (-ve slope of dashed line), but the approximately elliptical response is roughly symmetric around the line of constant stiffness.

Figure 5: *Test 2. Compliant behaviour with stiffness and damping: experimental results with $k_1 = 2.4$ Nm/deg (stiffness), $k_2 = 1$ Nm·s/deg (damping) and $k_3 \to \infty$ (no integral action). The joint was manually moved between the angles of approximately 20 and 40 deg and held at these levels for a short time between moves.*

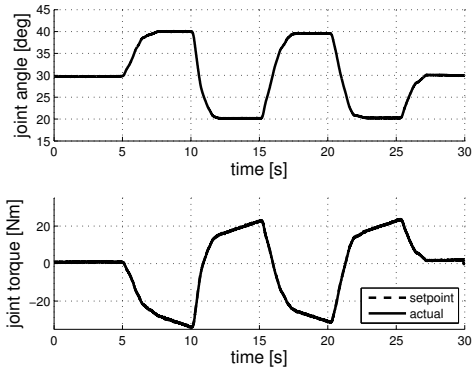

(a) Joint angle θ and torque τ_{mj}.

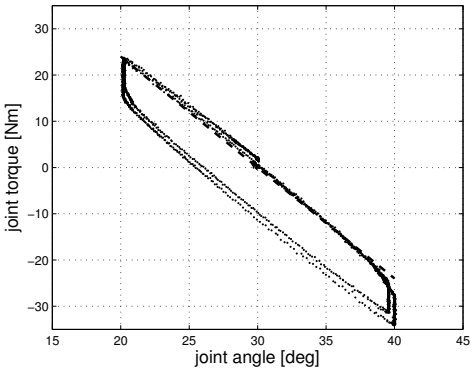

(b) Joint torque τ_{mj} vs. joint angle θ: clear deviation from a pure stiffness characteristic of 2.4 Nm/deg (-ve slope of dashed line).

Figure 6: *Test 3. Non-compliant behaviour due to integral action: experimental results with $k_1 = 2.4$ Nm/deg (stiffness), $k_2 = 0$ (no damping) and $k_3 = 4$ deg·s/Nm (integral action). The joint was manually moved between the angles of approximately 20 and 40 deg and held at these levels for a short time between moves despite the increasing motor-generated joint torque caused by integral action which had to be countered by the experimenter increasing his external disturbance torque d.*

tain the constant joint position. The impedance characteristic is substantially different from that of a stiffness (Figure 4(b)) or stiffness-damping compensator (Figure 5(b)): see Figure 6(b). This clearly demonstrates the non-compliant behaviour of the compensator with integral action.

The same compensator with integral action was used in the fourth test, but the experimental strategy was changed. The joint was moved initially to an angle of approximately 40 deg. At this angle, the joint torque had a value of approximately 30 Nm (Figure 7(a), lower graph). The experimenter then attempted to keep the torque at around this value, but to achieve this he had to allow the joint to move gradually back towards the neutral position of $\theta^* = 30$ deg (Figure 7(a), upper graph). The impedance characteristic again deviates considerably from that of a pure stiffness (Figure 7(b)), thus further illustrating the non-compliant nature of a compensator with integral action.

The first four tests were contrived to illustrate the concepts of compliance and non-compliance. The fifth and final test shows what happens in the more realistic situation when the reference angle θ^* has a profile which is similar to the ankle-angle profile of normal walking [5]: the compliant pure-stiffness control strategy still gives accurate reference tracking (Figure 8).

The behaviours we have seen can be further understood in terms of the load sensitivity functions (Eqs. (2)–(3)) by considering the Bode magnitude plots of $1/C(s)$ shown in Figure 9 for the three compensators used: the proportional (P) stiffness controller $C_p = 2.4$, the proportional-derivative (PD) stiffness-damping controller $C_{pd} = 2.4 + \frac{s}{0.1s+1}$ and

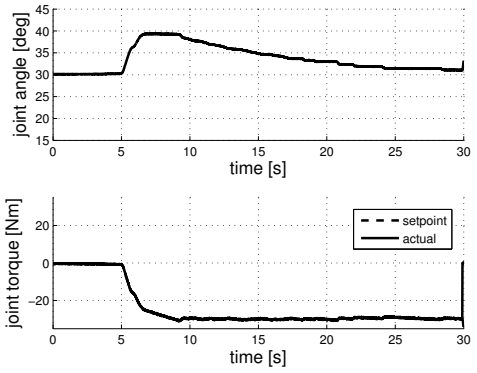

(a) Joint angle θ and torque τ_{mj}.

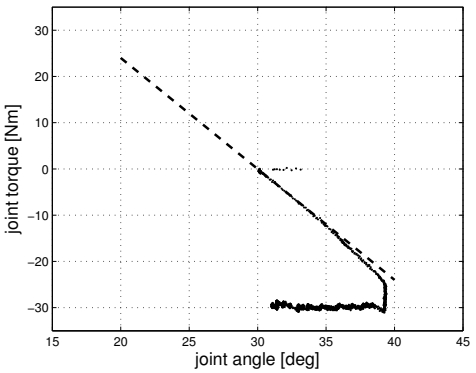

(b) Joint torque τ_{mj} vs. joint angle θ: clear deviation from a pure stiffness characteristic of 2.4 Nm/deg (-ve slope of dashed line).

Figure 7: *Test 4. Non-compliant behaviour due to integral action: experimental results with $k_1 = 2.4$ Nm/deg (stiffness), $k_2 = 0$ (no damping) and $k_3 = 4$ deg·s/Nm (integral action). The joint was manually moved to an angle of approximately 40 deg following which the experimenter allowed the joint to move back towards the neutral position of $\theta = 30$ deg while attempting to keep the torque magnitude at a value of around 30 Nm.*

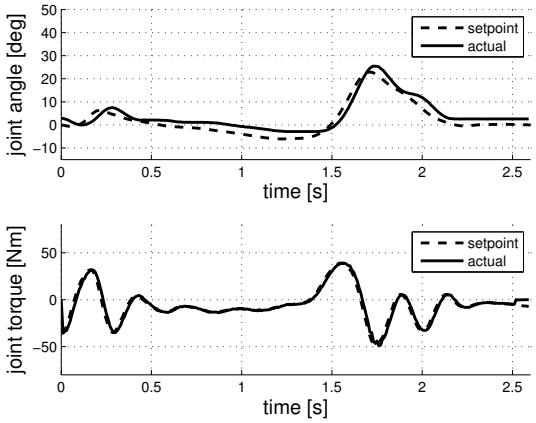

Figure 8: *Test 5. Ankle trajectory control. The reference/setpoint angle θ^* (dashed line, upper graph) has a profile similar to the joint-angle profile of normal walking. The lower graph shows the joint torque τ_{mj} and its setpoint τ^*_{mj}. Here, $k_1 = 2.4$ Nm/deg (stiffness), $k_2 = 1$ Nm·s/deg (damping) and $k_3 \to \infty$ (no integral action).*

the proportional-integral (PI) controller $C_{pi} = 2.4 + \frac{1}{4s}$. For the P and PD controllers the steady-state magnitude of $1/C$ is -7.6 dB ($= 20\log_{10}\frac{1}{2.4}$) so that the compliant stiffness characteristic with respect to external torque is achieved. For the PI controller the steady-state magnitude of $1/C$ is $-\infty$ dB ($= 20\log_{10}\frac{1}{\infty}$): the infinite steady-state controller gain makes the behaviour non-compliant.

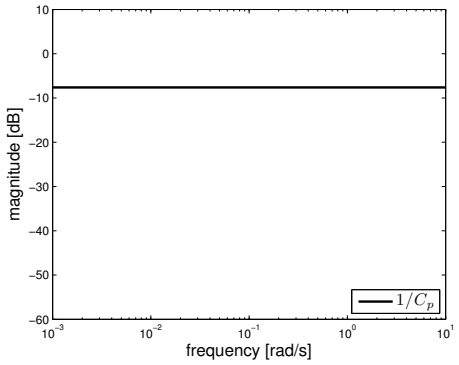

(a) $1/C_p$: this controller has stiffness only, and is just a P-controller.

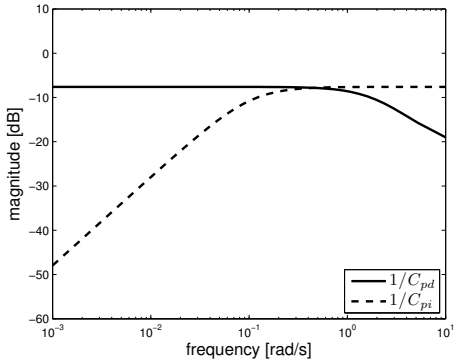

(b) $1/C_{pd}$: controller with stiffness and damping (PD-controller); $1/C_{pi}$: controller with proportional gain and integral action (PI-controller).

Figure 9: *Frequency-magnitude responses of the approximate torque disturbance transfer functions* $1/C$*:* $d \to \theta$*:* $G_{\theta d}(s) = \frac{P(s)}{1+C(s)P(s)} \approx \frac{1}{C(s)}$*, Equation (2). From Equation (3),* $\theta_{ss} \approx \lim_{\omega\to 0} |C(j\omega)|^{-1} d$.

Discussion

Rehabilitation robots in general and the ankle joint in particular can easily be packed in a morphological box; the problem of designing a rehabilitation robot lends itself well to the morphological way of thinking. Such devices are usually attached to, or at least used by, a human being and their form often mimics human biomechanical structures. The artificial ankle joint with its electromechanical components and its programmable control unit neatly matches the morphological control concept of farming out from a central processing unit — in this context, the human brain — computation and control structures to external materials and components. When one begins the design process in this world view the process and product can certainly be regarded as morphological.

But a traditional control engineering design process may also lead to a system which, in retrospect, can be painted with the morphological brush. The ankle joint control example shows that behaviour obtained on the basis of classical engineering concepts can be reinterpreted in terms more in tune with morphology. Engineering concepts for the design of automatic control systems have been around for a very long time [3]: they can provide a solid basis for design and analysis, and they do not preclude behaviour concepts to the fore in morphology.

In the end, the name given to your design process depends largely on the way you think about it: if you wish to design a morphological control system you simply start from ...

> *The Morphological Viewpoint: a morphological computation or control system is one which is designed from a morphological point of view.*

Bibliography

[1] K. J. Åström. Adaptive feedback control. *Proc IEEE*, 75(2):185–217, February 1987.

[2] K. J. Åström and R. M. Murray. *Feedback Systems*. Princeton University Press, 2008.

[3] H. W. Dickinson. *James Watt: craftsman and engineer*. Cambridge University Press, 2010.

[4] A. Esquenazi and A. Packel. Robotic-assisted gait training and restoration. *Am J Phys Med Rehabil*, 91(11 Suppl 3):S217–S231, Nov 2012. doi: 10.1097/PHM.0b013e31826bce18.

[5] J. Fang, H. Gollee, S. Galen, D. B. Allan, K. J. Hunt, B. A. Conway, and A. Vuckovic. Kinematic modelling of a robotic gait device for early rehabilitation of walking. *Proc Inst Mech Eng H*, 225(12):1177–1187, 2011.

[6] R. M. Füchslin, A. Dzyakanchuk, D. Flumini, H. Hauser, K. J. Hunt, R. H. Luchsinger, B. Reller, S. Scheidegger, and R. Walker. Morphological computation

and morphological control: steps towards a formal theory and applications. *Artificial Life*, 19(1), 2013.

[7] K. J. Hunt, H. Gollee, and R.-P. Jaime. Control of paraplegic ankle joint stiffness using FES while standing. *Med Eng Phys*, 23:541–555, October 2001.

[8] J. Martin, SJ. *The Jesuit Guide to Almost Everything.* Harper Collins, New York, USA, 2012.

[9] R. Pfeifer, M. Lungarella, and F. Iida. Self-organization, embodiment, and biologically inspired robotics. *Science*, 318:1088–1093, 2007.

[10] J. Stein. Robotics in rehabilitation: technology as destiny. *Am J Phys Med Rehabil*, 91(11 Suppl 3):S199–S203, Nov 2012. doi: 10.1097/PHM.0b013e31826bcbbd.

[11] J. G. Truxal. The concept of adaptive control. In E. Mishkin and L. Braun, editors, *Adaptive Control Systems*, chapter 1. McGraw-Hill, New York, USA, 1961.